Assessment of the tunable laser crystal $LiNbO_3:Cr^{3+}$

1993 J. Phys.: Condens. Matter 5 2041

(http://iopscience.iop.org/0953-8984/5/13/020)

J. Phys.: Condens. Matter 5 (1993) 2041–2044. Printed in the UK

Assessment of the tunable laser crystal $LiNbO_3:Cr^{3+}$

Yuanwu Qiu†‡

† China Centre of Advanced Science and Technology (World Laboratory), PO Box 8730, Beijing 100080, People's Republic of China
‡ Pohl Institute, Tongji University, Shanghai 200092, People's Republic of China

Received 30 June 1992, in final form 7 December 1992

Abstract. The electronic structures of Cr^{3+} ions on the Nb site and the Li site of $LiNbO_3$ were calculated under the actual site symmetry C_3 with the spin-polarized self-consistent-charge discrete variational X_α (SCC-DV-X_α) method. Special emphasis is placed on a discussion of the potential of $LiNbO_3:Cr^{3+}$ as a tunable laser crystal.

1. Introduction

The $LiNbO_3$:Nd laser was developed early in the 1960s. However, because of photorefractive damage caused by photovoltaic photorefractivity, its practicality is limited. Recently it was discovered that the photorefractive damage can be reduced by the addition of MgO to $LiNbO_3$ [1]. Thus the practicality of the $LiNbO_3$:Nd laser has been greatly improved. Because the $LiNbO_3$:Nd laser possesses the features of self-frequency-doubling and self-Q-switching, it has attracted much attention. Chromium-doped $LiNbO_3$ crystals possess a strong broad-band fluorescence; so it would add the extra feature of tunability to the $LiNbO_3$:Nd laser.

Michel-Calendini *et al* [2] calculated the electronic structure of Cr^{3+} ions in $LiNbO_3$ with the MS–X_α method applied to C_{3v} clusters representative of the different possible substitutional sites in the crystal host. In this paper, we calculated the electronic structure of Cr^{3+} ions on the Nb site and the Li site of $LiNbO_3$ under the actual site symmetry C_3 with the spin-polarized DV–X_α method and place special emphasis on a discussion of the potential of $LiNbO_3:Cr^{3+}$ as a tunable laser crystal.

2. Method of calculation

$LiNbO_3$ is rhombohedral with the space group $R3c$ (C_{3v}^6). The lattice constants are $a_H = 5.148\,29$ Å and $c_H = 13.8631$ Å [3]. There are six formula units per hexagonal (two per rhombohedral) unit cell. The structural parameters are listed in table 1.

The Nb ion and the Li ion are both situated within the oxygen octahedra of C_3 symmetry and are distributed alternately along the C_3 axis of the crystal. The top and the bottom oxygen triangles of the octahedron are rotated from each other by an angle α. For the Li octahedron, $\alpha = 3°49'$, while the Nb octahedron has $\alpha = 41'$. In other words, Li is situated in a very distorted octahedron. The cation–oxygen distances of Nb–O and Li–O are 1.889 and 2.112 Å for the former and 2.068 and 2.238 Å for the latter.

0953-8984/93/132041+04$07.50

Cr^{3+} ions are found to substitute both for Li and for Nb sites by ESR [4], ENDOR [5] and simulations [6]. It is also predicted that C^{3+} ions at the Li site are probably displaced towards a more centrosymmetric position on the *c* axis. However, this hypothesis should be further confirmed [6]. The optical properties of the Cr^{3+} ion on the Nb site and the Li site in $LiNbO_3$ can be obtained by calculations of the ion cluster $(CrO_6)^{9-}$ formed by the luminescent centre Cr^{3+} and the six nearest oxygen ions O^{2-}. Calculations were performed for the cluster $(CrO_6)^{9-}$ by the spin-polarized SCC-DV-X_α method. 3000 discrete points were taken. The frozen-core model was adopted. 1s–4s were taken as the numerical basis sets for Cr^{3+} where 1s–3p were frozen, and 1s–2p as those for O^{2-} where 1s was frozen. All calculations were performed on the Siemens 7.570-C computer at Tongji University.

3. Results and discussion

3.1. One-electron energy levels

The calculated one-electron energy levels of the cluster $(CrO_6)^{9-}$ for the Nb site and the Li site can be roughly divided into five regions:

(1) O^{2-}_{2s} non-bonding levels with energy values between −14.0 and −10.0 eV;

(2) bonding levels formed by Cr^{3+}_{3d} and O^{2-}_{2p} with energy values between −5.0 and −1.0 eV;

(3) O^{2-}_{2p} non-bonding levels with energy values between −1.0 and 1.0 eV;

(4) Cr^{3+}_{3d} crystal-field levels with energy values between 5.0 and 10.0 eV;

(5) antibonding levels formed by Cr^{3+}_{4s} and O^{2-}_{2p} with energy values between 12.0 and 14.0 eV.

The 3d one-electron energy levels are shown in figure 1.

It is shown that the energies of 3d levels and the interval between the 3d levels and the O^{2-}_{2p} non-bonding levels for the Nb site are greater than those for the Li site. The reason is that the cation–oxygen distance of the Nb site is smaller; so the interaction between the 3d levels and the ligand levels is greater. Thus the 3d levels are pushed up farther. The one-electron eigenvalues of the 3d levels are listed in table 2.

Table 1. Structural parameters of $LiNbO_3$.

Atom	x	y	z
Nb	0.0	0.0	0.0
O	0.0492	0.3446	0.0647
Li	0.0	0.0	0.2829

3.2. Energy differences between the $^4T_2$ and ^2E states

For the purpose of classifying materials and connecting the nature of the emission band to the ligand field, Kenyon *et al* [7] introduced the parameter Δ which represents the energy difference between the $^4T_2$ and ^2E states and noted that materials of importance for tunable lasers must belong to the intermediate-field ($\Delta \simeq 0$) or low-field ($\Delta < 0$) category. Experimentally Δ is measured from the positions of the zero-phonon $^4T_2$ transition and the ^2E band. In our previous papers [8, 9], we discussed the

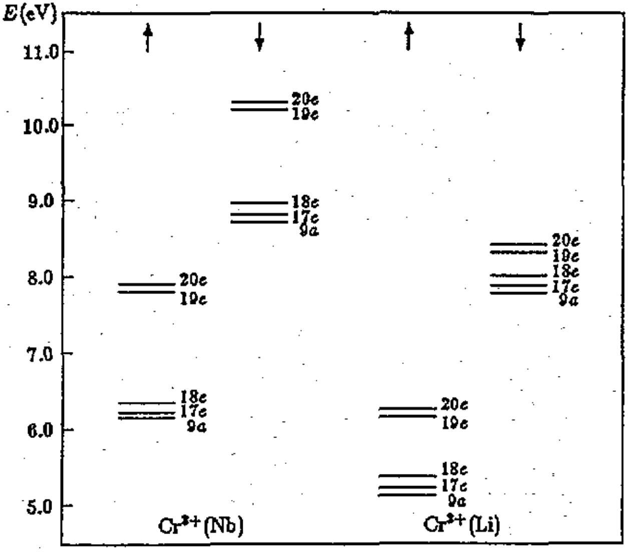

Figure 1. 3d one-electron energy levels of the cluster $(CrO)_6)^{9-}$.

Table 2. One-electron eigenvalues of the 3d energy levels.

	Eigenvalue (eV)			Eigenvalue (eV)	
	Cr^{3+} (Nb)	Cr^{3+} (Li)		Cr^{3+} (Nb)	Cr^{3+} (Li)
20e↑	7.9083	6.4240	20e↓	10.3922	8.6283
19e↑	7.8677	6.2746	19e↓	10.2703	8.5679
18e↑	6.2032	5.2127	18e↓	8.8872	7.9465
17e↑	6.1959	5.2022	17e↓	8.8793	7.9357
9a↑	6.1308	5.1298	9a↓	8.7202	7.8141

positions of the doublet terms of the configuration t_{2g}^3 using the information provided by the spin-polarized X_α calculation under lower site symmetry. This enables us to calculate the energies of the ^2E state as well as those of the $^4T_2$ state of Cr^{3+} in various crystal hosts, and to obtain Δ.

In order to calculate the energy difference between the $^4T_2$ and ^2E states, Slater's [10] transition state theory is used to calculate the transition energies of the 18e↑–19e↑, 9a↑–19e↑, 9a↑–20e↑, 17e↑–9a↓ and 18e↑–9a↓ transitions. The averaged value of the three former transition energies is the energy of the $^4T_2$ state, and that of the two latter transition energies is the energy of the ^2E state. The calculated values of the energies of the $^4T_2$ and ^2E states and their experimental values [11], together with the calculated results of Michel-Calendini *et al* [2] are listed in table 3. It is seen that our calculated results are closer to the experimental results than those in [2] are. The muffin-tin potential approximation used in the MS–X_α method is inadequate for quantitative description of detailed electronic states mainly because a constant potential is used in the intersphere region. On the other hand, the DV–X_α method does not use the muffin-tin approximation but uses the more accurate SCF potential and is superior to the MS–X_α method.

It is reasonable that the zero-phonon $^4T_2$ state lies 183 cm^{-1} higher than the ^2E state for the Nb site, while the zero-phonon $^4T_2$ state lies 3410 cm^{-1} lower than the ^2E state for the Li site, since the cation–oxygen distance of the Li site is substantially greater than that of the Nb site and is in the low-field region of the Tanabe–Sugano [12] diagram where the $^4T_2$ state lies lower than the ^2E state. It is

Table 3. Calculated and experimental energies of the $^4T_2$ and ^2E states.

	O_h	C_3	Transition	Energy (cm^{-1})	Averaged (cm^{-1})	Experimental [11] (cm^{-1})	Calculated [2] (cm^{-1})
Cr^{3+} (Nb)	$^4T_2$	E	$9a\uparrow - 20e\uparrow$	14 443	14 019	13 645	16 374
	$^4T_2$	E	$9a\uparrow - 19e\uparrow$	14 139			
	$^4T_2$	A	$18e\uparrow - 19e\uparrow$	13 474			
	^2E	E	$18e\uparrow - 9a\downarrow$	13 882	13 836	13 686	17 019
	^2E	E	$17e\uparrow - 9a\downarrow$	13 790		13 616	
Cr^{3+} (Li)	$^4T_2$	E	$9a\uparrow - 20e\uparrow$	10 961	10 395		6865
	$^4T_2$	E	$9a\uparrow - 19e\uparrow$	10 473			
	$^4T_2$	A	$18e\uparrow - 19e\uparrow$	9751			
	^2E	E	$18e\uparrow - 9a\downarrow$	13 867	13 805	13 754	20 004
	^2E	E	$17e\uparrow - 9a\downarrow$	13 743		13 686	

also reasonable that the trigonal field splittings of the $^4T_2$ and ^2E states (1210 cm^{-1} and 124 cm^{-1}, respectively) for the Li site are greater than those (969 cm^{-1} and 92 cm^{-1}, respectively) for the Nb site, since the Li site is situated in a substantially more distorted octahedron than the Nb site is. The calculated results indicate that the crystal $LiNbO_3:Cr^{3+}$ ($\Delta = 183$ cm^{-1}) belongs to the intermediate-field category, which the crystal GSGG:Cr^{3+} ($\Delta = 50$ cm^{-1}) [13], one of the best tunable laser crystals, also belongs to. In the intermediate-field regime, the closeness of the $^4T_2$ and ^2E states enables the population in the ^2E state to transfer into the $^4T_2$ state through thermal excitation at room temperature, and from the $^4T_2$ state the phonon-assisted broad-band fluorescence which is necessary for tunability of a laser is emitted. The metastable ^2E state acts as an energy reservoir to favour room-temperature operation of the tunable solid state laser.

In summary, the crystal $LiNbO_3:Cr^{3+}$ is a candidate for a room-temperature tunable solid state laser, provided that the dynamical behaviours of the Cr^{3+} ion in $LiNbO_3$ also support this conclusion. Therefore further calculations of transition probabilities should be performed with respect to its potential as a tunable laser crystal.

Acknowledgment

This project was supported by the National Natural Science Foundation of China.

References

[1] Zong G, Jian J and Wu Z 1980 *Proc. 11th Int. Quantum Electronics Conf.* (New York: IEEE) p 631

[2] Michel-Calendini F M, Moretti P and Chermette H 1987 *Cryst. Latt. Defects Amorph. Mater.* **15** 65

[3] Abrahams S C, Reddy J M and Berstein J L 1966 *J. Phys. Chem. Solids* **27** 997

[4] Malovichko G I, Cravero I, Polgar K and Capelletti R 1986 *Sov. Phys.–Solid State* **28** 553

[5] Corradi C, Sothe H, Spaeth J M and Polgar K 1991 *J. Phys.: Condens. Matter* **3** 1901

[6] Michel-Calendini F M, Bellafouh K and Daul C 1992 *Ferroelectrics* **125** 271

[7] Kenyon P T, Andrews L, McCollum B and Lempicki A 1982 *IEEE J. Quantum Electron.* **QE-18** 1189

[8] Qiu Y and Zhu J K 1989 *Z. Phys.* B **75** 447

[9] Qiu Y, Tang X and Zhu J K 1990 *Z. Phys.* B **78** 271

[10] Slater J C 1972 *Adv. Quantum Chem.* **6** 1

[11] Jia W, Liu H, Knutson R and Yen W M 1990 *Phys. Rev.* B **41** 10 906

[12] Tanabe Y and Sugano S 1954 *J. Phys. Soc. Japan* **9** 766

[13] Struve B and Huber G 1982 *Appl. Phys.* B **36** 195